2008 IEEE International Conference on
Robotics and Automation
Pasadena, CA, USA, May 19-23, 2008

Bilateral Telemanipulation of a Flexible Catheter in a Constrained Environment

J. Jayender **M. Azizian** **R. V. Patel**

Department of Electrical and Computer Engineering,
University of Western Ontario,
London, ON N6A 5B9, Canada
jjagadee@uwo.ca, mazizian@uwo.ca, rajni@eng.uwo.ca

Abstract— **This paper describes some novel research results on bilateral teleoperation of a flexible catheter in a constrained environment. The dynamics of the catheter in a constrained environment is highly nonlinear and is affected by a large number of factors such as friction, flexibility of the catheter, force of insertion, shape and size of the catheter, etc. As a result, the distal end of the catheter almost never follows the actuated end of the catheter which could cause fatigue to the clinician/user attempting to insert the catheter in a blood vessel. In addition, there is a time delay of up to 0.8 second before the distal end of the catheter advances after the near end is actuated. This delay is sufficient to cause instability in the control loop. We have developed a teleoperation framework using wave variables to perform robot-assisted catheter insertion in a constrained environment while reflecting the forces at the tip of the catheter to the clinician. Experimental results showing the effect of different factors such as the velocity and stroke length of insertion on the delays introduced in control loop and errors between the master and slave position are included. To the best of our knowledge, this work is among the first to attempt to provide an understanding of the effects of various factors on the flexing of the catheter. In addition, master-slave insertion of a catheter instrumented with Shape Memory Alloys (SMA) has also been performed and the results are included in this paper.**

Index Terms— **Flexible link, bilateral teleoperation, wave variables, robot-assisted catheter insertion, hybrid impedance control, active catheter, shape memory alloy actuators, real-time catheter tracking.**

I. Introduction

This paper addresses a novel robot control problem in which a highly flexible link with no actuators along its length is guided from one end of the link through a constrained environment. One such application is that of a catheter being guided through the lumen of the blood vessel to perform angioplasty. Angioplasty is a minimally invasive procedure that involves the insertion of a catheter into a blood vessel for removal of blockages in blood flow.

The dynamics of the catheter within a constrained environment is highly non-linear due to the frictional forces acting along the length of the catheter and the high flexibility of the catheter. As a result, the tip of the catheter may not follow the motion of the actuated end of the catheter. The catheter may flex within the constraints without any forward motion of its distal end. In addition, frictional forces acting along the length of the catheter may cause stiction and prevent the tip from moving forward. The friction may be of a dynamic nature at a few points along the length of the catheter and may be of a static nature at other points along the catheter. Due to this fact and the highly flexible nature of the catheter, energy may be stored within the catheter in the form of spring-like potential energy and may be released at an instant when the static friction is overcome, thereby causing an extremely jerky motion of the tip of the catheter. This can cause considerable difficulty in smoothly advancing the tip of the catheter inside the body. The actuated end may have to move nearly twice as much to advance the far end of the catheter. In addition, the actuation at the distal end takes place following a significant time delay after the application of force at the actuating end. The delay is dependent on a number of factors including the structure of the catheter and the friction acting along its length. This delay may also induce instability in the control loop while performing bilateral teleoperation.

In this paper, we have developed a wave variable based bilateral teleoperation framework to perform master-slave catheter insertion for application in angioplasty. The bilateral teleoperation framework maintains stability even in the presence of time delays resulting from the dynamics associated with catheter insertion. In addition, the tip of the catheter follows the reference generated by the haptic device while the force at the tip of the catheter is reflected to the haptic device, thereby compensating for the flexing in the catheter and providing the clinician with a transparent and reliable way of advancing the catheter into the body. It should be noted that the control developed in this paper is a model-free algorithm and a more detailed model would be necessary to develop an accurate control irrespective of the velocity or the stroke length of insertion, geometry of the test-bed or initial orientation of the robot. In this paper, as a first step, in addition to developing the bilateral teleoperation framework, we have also performed a number of experiments on a highly flexible catheter to better understand the effect of velocity/force of insertion, stroke length of insertion and geometry of the path, on the amount of flexing of the catheter

This work was supported by funds from the Natural Sciences and Engineering Research Council (NSERC) of Canada under Grant RGPIN-1345 and by an infrastructure grant from the Canada Foundation for Innovation awarded to the University of Western Ontario (R. V. Patel).

(measured in terms of deadband delay and error between the master and slave). This data will eventually help us develop a model based on the experimental data, which we believe would be more suitable for real-time control purposes over the present physics-based simulation models developed in the literature.

Kukuk and Geiger in [1] have studied a model for flexible instruments inserted into tubular structures. This model is based on the recursive enumeration of all possible shapes of the long flexible instrument (e.g. a catheter) and subsequently filtering them according to given mechanical and physical constraints. Although the complexity of such a problem is very high, Kukuk and Geiger [1] have used the constraints as well as some approximations to limit the number of possible solutions and reduce the complexity. Most of the work on modeling long flexible instruments (such as wires, catheters, guidewires and endoscopes) inserted in constrained environments involves physics-based simulations using different methods [2], [3]. It is not easy to use these physics-based simulated models for real-time control of the flexible instrument. In this paper, we have presented some experimental results which can be used to get a better understanding of this problem as well as to evaluate the overall performance of bilateral teleoperation.

In addition, we have also instrumented the catheter with Shape Memory Alloy actuators to help guide the catheter through the vasculature. A novel image processing algorithm [4] has also been developed to track the tip of the catheter as it is inserted into the body. The algorithm provides information to the clinician on the position of the tip of the catheter with respect to the vasculature, thereby aiding the clinician in varying the insertion velocity as the catheter approaches or leaves junctions.

II. Wave variables based teleoperation

Bilateral teleoperation is the ability of an operator to manipulate a robot at a distance while receiving force feedback from the interaction between the robot and its environment. In the case of performing robot-assisted catheter insertion, the clinician applies a force on a master unit - a haptic device (force reflecting joystick) which produces a displacement. The displacement of the haptic device is then transmitted to the robot over a communication channel to command it to insert the catheter remotely. The force felt at the tip of the catheter is communicated back to the operator and is fed as torques to the motors of the haptic device. It has been shown in the literature on minimally invasive surgery that the ability of the clinician to feel the interaction forces between surgical tools and tissue in addition to visual feedback increases the accuracy of the procedure, while decreasing the possibility of injuring or rupturing the blood vessels [5]. However, time delays introduced into the control loop either through the communication channel or through the slave dynamics can eventually lead to a degradation of the performance of the procedure and/or instability. In our case, since the teleoperation was performed over a local network, the time delay introduced in the communication channel was minimal. The major contribution to time delays was introduced by the high flexibility of the catheter and the non-linear dynamics of the Shape Memory Alloys (SMA) actuators.

The wave variables based approach proposed by Niemeyer and Slotine [6] is a modification of the passivity based teleoperation suggested by Anderson and Spong [7]. Instead of exchanging the power variables, the master and slave subsystems exchange what are called wave variables. For constant time delays, the wave variables are identical to the formulation given in [7]. However, the advantage of using the wave variables is that the force and velocity are uniquely encoded into the wave variables without explicitly defining the overall scheme as an impedance or an admittance based system. This encoding of the power variables into the wave variables also make them applicable to nonlinear systems and creates robustness to arbitrary time delays, making it an attractive approach to perform bilateral teleoperation for robot-assisted catheter insertion.

III. Wave variables architecture

The bijective transformation from power variables $(\mathbf{F}, \dot{\mathbf{x}})$ to the wave variables $(\mathbf{u}, \mathbf{v})$ is given by,

$$\mathbf{u} = \frac{b\dot{\mathbf{x}} + \mathbf{F}}{\sqrt{2b}} \qquad \mathbf{v} = \frac{b\dot{\mathbf{x}} - \mathbf{F}}{\sqrt{2b}} \tag{1}$$

where $\mathbf{u}$ is used to denote the forward moving wave, $\mathbf{v}$ to denote the returning wave and b the characteristic impedance of the transmission line. In addition, the parameter b can also be used as a tuning parameter to obtain a tradeoff between the velocity of operation and the forces reflected. Since this transformation is bijective, no information is lost and the power variables can be uniquely computed from the wave variables as follows,

$$\dot{\mathbf{x}} = \frac{1}{\sqrt{2b}}(\mathbf{u} + \mathbf{v}) \qquad \mathbf{F} = \sqrt{\frac{b}{2}}(\mathbf{u} - \mathbf{v}) \tag{2}$$

As mentioned earlier, the delays introduced in the dynamics of the slave subsystem can be assumed to arise from the communication channel. By encoding the power variables in this way, the system is stabilized regardless of the delay. Both the master and slave have separate controllers. The equations governing the transmission of the wave variables are given by,

$$\mathbf{u}_s(t) = \mathbf{u}_m(t - T) \tag{3}$$

$$\mathbf{v}_m(t) = \mathbf{v}_s(t - T) \tag{4}$$

The slave PD controller ensures that the slave velocity (in this case the catheter tip position) is forced to track the desired velocity generated from the wave variables as follows,

$$\dot{\mathbf{x}}_{sd} = \frac{\sqrt{2b}\mathbf{u}_s + B\dot{\mathbf{x}}_s + K(\mathbf{x}_s - \mathbf{x}_{sd})}{B + b} \tag{5}$$

where $\mathbf{x}_s$ is the position of the tip of the catheter obtained from the image processing algorithm, $\dot{\mathbf{x}}_s$ is the velocity of

the catheter tip obtained by a first order difference equation, $\mathbf{x}_{sd}$ and $\dot{\mathbf{x}}_{sd}$ are the desired tip position and velocity, $\mathbf{u}_s$ is the incoming wave at the slave side, b is impedance tuning parameter and B and K are the velocity and position gains respectively. It should be carefully noted here that the catheter (and not the robot) is being considered as the slave subsystem.

The driving force or the coordinating force is calculated as

$$F_s = -B(\dot{\mathbf{x}}_s - \dot{\mathbf{x}}_{sd}) - K(\mathbf{x}_s - \mathbf{x}_{sd}) \tag{6}$$

The return wave to the master is computed by the following equation,

$$\mathbf{v}_s = \mathbf{u}_s - \sqrt{\frac{2}{b}}\mathbf{F}_s \tag{7}$$

On the master side, the force reflected to the haptic device is given as,

$$\mathbf{F}_m = b\dot{\mathbf{x}}_m - \sqrt{2b}\mathbf{v}_m \tag{8}$$

and the reflected wave to the slave is computed as,

$$\mathbf{u}_m = \sqrt{2b}\dot{\mathbf{x}}_m - \mathbf{v}_m \tag{9}$$

It should be noted here that the dynamics of the slave, i.e, the catheter is highly complex, depending on a number of factors such as the material of the catheter, geometry of the path, static and dynamic friction coefficients, force of insertion, diameter of the vessel and the catheter, initial orientation of insertion, fluid flow etc. In addition, the catheter is indirectly manipulated using a robot at the remote site of insertion. Due to the high flexing of the catheter inside the arteries, the robot end effector velocity is not necessarily equal to the velocity of the tip of the catheter. The robot velocity is generated based on the catheter tip position and velocity as given by the following equation,

$$\dot{\mathbf{x}}_{rd} = K_p(\mathbf{x}_{sd} - \mathbf{x}_s) + K_d(\dot{\mathbf{x}}_{sd} - \dot{\mathbf{x}}_s) + K_i \int (\mathbf{x}_{sd} - \mathbf{x}_s)dt \tag{10}$$

where $\dot{\mathbf{x}}_{rd}$ is the desired robot end effector velocity. This desired velocity is provided to the Augmented Hybrid Impedance Control (AHIC) scheme for the robot, developed in [8].

IV. Augmented Hybrid Impedance Control

An Augmented Hybrid Impedance Control (AHIC) scheme has been implemented on a Mitsubishi PA 10-7C robot. The AHIC module combines impedance control and hybrid position/force control into one scheme. To perform bilateral teleoperation, the desired Cartesian velocity ($\dot{\mathbf{x}}_{rd}$) is provided to the AHIC scheme while performing Cartesian control in all directions. A brief overview of the algorithm is given below.

In the AHIC scheme, there are basically two control loops - the outer loop generates the position and force profiles that have to be tracked in real-time and determines the desired Cartesian acceleration that is fed to the inner loop. The inner loop converts the Cartesian acceleration to a joint level acceleration and the desired torques for each of the links are generated to track both the desired position and force profiles. The block diagram is given in Figure 1.

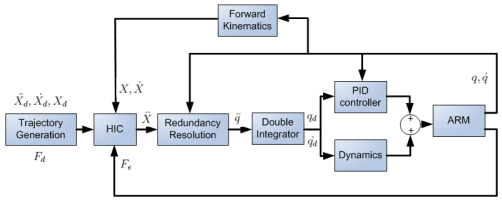

Fig. 1. Augmented Hybrid Impedance Control

1) Augmented Hybrid Impedance Control Module: The AHIC module is defined by the following equation:

$$\ddot{X}^t = M_d^{-1}[-F_e + (I - S)F_d - B_d(\dot{X} - S\dot{X}_d) - K_d S(X - X_d)] + S\ddot{X}_d \tag{11}$$

where M_d and B_d are the desired mass and damping parameters, F_d and F_e are the desired force and environment contact forces, X, $\dot{X}$ and $\ddot{X}$ are the Cartesian positions/orientations, and the corresponding velocities and accelerations respectively. The matrix $\mathbf{S}$ denotes the selection matrix which defines the force and position controlled subspaces.

2) Redundancy Resolution: The inner loop which consists of the redundancy resolution module converts the Cartesian acceleration to a desired joint level acceleration which is provided to the joint-based controller. Since the Mitsubishi PA 10-7C robot has 7 DOFs, the Jacobian is not square. As a result an additional task, which consists of joint-limit avoidance for the redundant joint S3, is included to make the Jacobian square [9]. A damped least-squares solution at the acceleration level is implemented to damp out the joint velocities in the null-space of the Jacobian as given by the following equation:

$$\ddot{\theta} = [J_e^T W_e J_e + J_c^T W_c J_c + W_v]^{-1}[J_e^T W_e(\ddot{X}^t - \dot{J}_e\dot{\theta}) + J_c^T W_c(\ddot{Z}) - W_v\lambda\dot{\theta}] \tag{12}$$

where J_e and J_c are the Jacobian matrices corresponding to the primary and the secondary tasks, W_e and W_c are weight matrices, W_v is the singularity robustness factor and λ is the velocity damping factor.

The joint accelerations are integrated to obtain the desired joint velocities and positions and fed to the joint control module after canceling the gravity term.

3) Joint based controller: Each of the 7 joints is controlled to follow a certain desired trajectory. The dynamic model for a rigid-link manipulator is given by:

$$\tau = M(\theta)\ddot{\theta} + V(\theta, \dot{\theta}) + G(\theta) \tag{13}$$

where $M(\theta)$ is the mass matrix, $V(\theta, \dot{\theta})$ is the vector of Coriolis and centrifugal terms and $G(\theta)$ is the vector of gravity terms. For medical robots, the joint velocities and

accelerations are generally quite small and therefore the $V(\theta, \dot{\theta})$ terms can be assumed to be negligible. The gravity terms are obtained in closed-form.

V. Experimental results using an unactuated catheter

For the first set of experiments, to study the effect of various factors on the amount of flexing, we have performed robot-assisted insertion of an unactuated catheter in a test-bed. The testbed consists of vinyl tubes of varying diameters (3.0mm, 4.5mm and 6.0mm internal diameter). The diameters of the tubes chosen are smaller than the normal size of the femoral artery, which is 8.75mm $\pm$ 2.11mm [10], [11]. The bending angles and radii of the tubes are close to those of arteries in the human body to make the test-bed as realistic as possible for a proof-of-concept.

A. Insertion at constant master velocity

In the first set of experiments, we study the flexing of the catheter as it is inserted into the test-bed. The stroke length of the robot's end-effector is kept constant throughout the experiment. In addition, the haptic device is removed from the loop and replaced with a constant master velocity of $7mm/sec$. The experiments were repeated 10 times, keeping the parameters constant, to obtain reliable predictions by looking at the ensemble averages of the results.

Figure 2(a) shows the ensemble averaged maximum tracking error between the master and slave as a percentage of the master reference, and the difference between the maximum robot end-effector and the catheter tip movements as a percentage of the slave movement is shown in Figure 2(b). As can be seen in Figure 2(a), the tracking error between the master and the slave varies from 4 to 13% of the master reference which proves that the bilateral teleoperation provides good tracking. The difference between the maximum robot end-effector and the catheter tip movements as shown in the Figure 2(b) varies between 57 to 126%. This difference is mainly caused by the flexing of the catheter and by the frictional forces acting along the catheter.

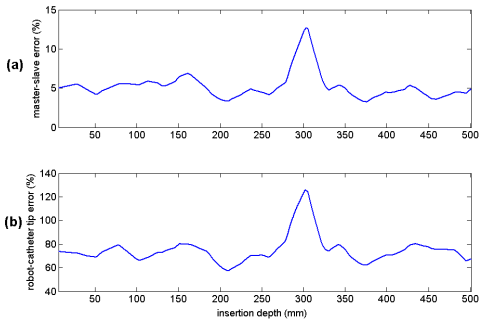

Fig. 2. (a) Ensemble averaged maximum master-slave tracking error (percentage of the peak master reference) vs. insertion depth (b) Ensemble averaged difference between the maximum robot end-effector and catheter tip movements (percentage of the maximum slave movements) vs. insertion depth

Figure 3 shows the ensemble averaged deadband vs. insertion depth. The deadband is the time it takes for the tip of the catheter to start moving after the master starts moving. There are four main factors that affect the deadband:

- vision tracking delay (constant, less than 0.1 seconds)
- network delay (negligible)
- stiction along the contact points between the catheter and the tube
- flexing of the catheter

As the delay caused by vision tracking is constant and is a small percentage of the total deadband (less than 15%) and the network delay is negligible, we can conclude that the main factors causing the deadband delay are stiction and flexing. Stiction depends on the number of contact points between the catheter and the tube, the curvatures of both the catheter and the tube at the points of contact, physical properties of the tube and the catheter and the friction coefficients. Stiction can be modeled as a semi-static effect. The deadband delay varies between 0.66 and 0.87 seconds with a standard deviation between 0.01 and 0.065 seconds over 10 ensembles, proving the reliability of the results.

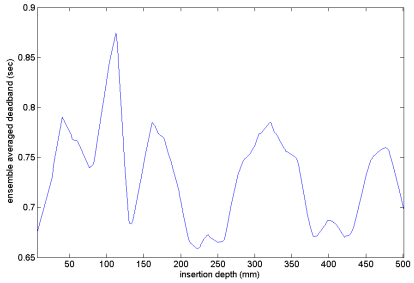

Fig. 3. Ensemble averaged deadband (sec) vs. insertion depth (mm)

In Figure 4 the average force of insertion is shown vs. the insertion depth. The average force of insertion increases as the catheter advances into the test-bed due to an increase in friction acting along the length of the catheter.

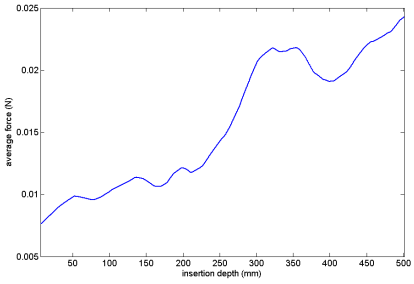

Fig. 4. Ensemble averaged force of insertion (N) vs. insertion depth (mm)

B. Insertion at variable master velocity

In the next set of experiments, the flexing of the catheter was observed as a function of the master velocity. For each insertion performed, the velocity of the master device was kept constant. Several such experiments were performed by varying the master velocity from $3mm/sec$ to $7mm/sec$. The mean deadband delay was measured to be 0.73 seconds

with a standard deviation of $38ms$. The wave variable architecture maintains stability even in presence of these delays and reflects the forces on the catheter tip to the haptic device. The average master slave error over the entire insertion is within $\pm 10\%$ of the master reference for different master velocities.

C. Insertion at variable robot end-effector stroke lengths

In this set of experiments, the unactuated catheter was inserted into the test-bed with varying stroke lengths of the robot's end-effector. It was observed that the mean deadband delay is 0.76 second and the standard deviation is $63ms$ for a variation in stroke length from 12mm to 30mm.

Figure 5 shows the average master slave error over the entire insertion plotted against the stroke length. The graph shows that the average master-slave error is lower for higher stroke lengths. This is quite expected since the flexing of the catheter is more pronounced for lower stroke lengths, resulting in greater master-slave error.

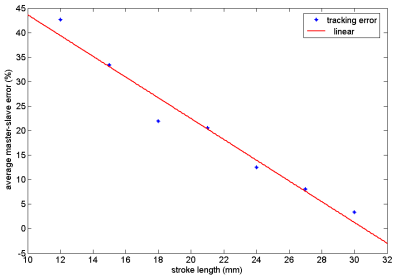

Fig. 5. Average master-slave tracking error (percent) vs. stroke length (mm) and linear regression of the data

VI. Experimental results using an actuated catheter

In these experiments, an active catheter is inserted into the test-bed using a haptic device. The catheter has been instrumented with SMA actuators to control the orientation of the distal end of the catheter. The catheter has also been instrumented with 3 strain gauges to measure the forces acting on the tip of the catheter. A similar wave variable architecture has been developed to independently control the orientation of the catheter while reflecting the forces on the tip of the catheter to the haptic device. The control is switched between the robot and the active catheter at junctions and the target on the clinician's command.

The user inserts the active catheter into the test-bed using the haptic device. The overhead camera, which mimics the X-ray imaging system, shows the progress of the catheter inside the test-bed. The image processing algorithm determines the tip position and overlays it with the images obtained from the camera to provide the clinician with a precise knowledge of the position of the catheter with respect to the tubes. In addition, the image processing algorithm also provides the user with indications to control the stroke length provided from the haptic device - away from the bifurcations, the algorithm provides normal stroke length command; close to the junctions the algorithm recommends to the user to reduce the stroke length; at the junction, it provides the user with the necessary the information to stop insertion and bend the catheter in the desired direction. Images obtained from a secondary camera also provide the user with visual information about the position of the end-effector of the robot with respect to the port of entry on the test-bed.

In the experiments performed here, the user remotely commanded the robot to insert the catheter into the test-bed. During the test, the user was sufficiently isolated from the robot and the test-bed and operated the robot and the catheter using only the images provided to him/her, thereby mimicking an actual remotely controlled master-slave catheter insertion. The path consists of two junctions, at the first the user has to bend the catheter to the right and at the second the user has to bend it to the left. The overall path length from the point of entry to the target is roughly about 1.7m. The results of the experiment are shown in Figure 6.

The user performed bilateral teleoperation and inserted the catheter into the test-bed, while the forces at the tip of the catheter were reflected to the stylus of the haptic device. As seen in Figure 6 region a (hereafter denoted as Figure 6:a), the user inserted the catheter into the test-bed with the maximum possible stroke. The control algorithm ensured that the tip of the catheter followed the reference generated by the haptic device. Figure 6(i) shows the position of the end-effector along with the position of the master and the tip of the catheter. Figure 7 shows a magnified view of the positions of the master, the robot end-effector and the catheter tip in region (a) of Figure 6. It can be seen that the catheter tip followed the reference generated by the haptic device quite accurately. The robot end-effector motion is nearly 50% higher than the catheter tip position in order to compensate for the flexing in the catheter. The figure also shows a significant delay in advancing the distal end of the catheter due to the frictional forces and high flexibility of the catheter.

Close to the junctions, the user reduced the stroke length using the haptic device. The image processing algorithm tracked the tip of the catheter and provided the desired suggestions to the user based on the proximity of the catheter from the junction. At the junction (Figure 6:c&h), the user was informed by the image processing algorithm to stop inserting the catheter. On pressing a key, the robot was disabled and the haptic device now controlled the active catheter. The user commanded the catheter to bend in the desired direction while the force exerted on the tip of the catheter was reflected to the stylus of the haptic device. Once the catheter reached the desired orientation, the user re-activated the robot to continue insertion of the catheter into the desired branch, as shown in Figure 6:(d)&(j). The user then waited for the actuators on the catheter to cool and regain their original shape before resuming normal insertion, as shown in Figure 6:(e)&(k). The force of insertion for the entire procedure is shown in Figure 6(ii).

The mean master-slave error was 9.72% of the master reference with a standard deviation of 0.1475%. It can be

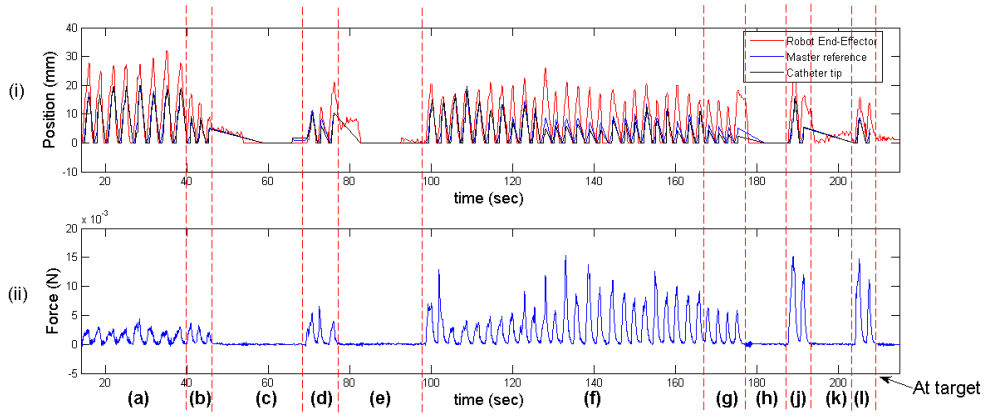

Fig. 6. Experimental results: (i) shows the master (haptic device), slave (catheter tip) and robot end-effector position vs. time during catheter insertion (ii) shows the force of insertion measured at the robot end-effector along the direction of insertion.
Different phases of insertion are shown as: (a) normal insertion before the first branch, (b) slow-down before the first branch, (c) no insertion, catheter bends at junction (d) insertion after bending is complete at the first junction, (e) wait for SMA actuators to cool (f) normal insertion before the second branch, (g) slow-down before the second branch, (h) no insertion, catheter bends at junction (j) insertion after bending is complete at the second junction, (k) wait for SMA actuators to cool (l) normal insertion before the target

observed from the results that both overshoot and undershoot occur while the catheter tip tracks the master reference, thereby proving the non-linear nature of the dynamics of catheter insertion. The mean difference between the end-effector motion and the catheter tip motion is 106.11% of the catheter tip motion, reaching a maximum around 600% near the second junction. The relatively large motion of the end-effector compared to the catheter tip is to compensate for the flexing of the catheter within the tubes. The deadband delay is variable and lies between 0.4 and 0.9 seconds.

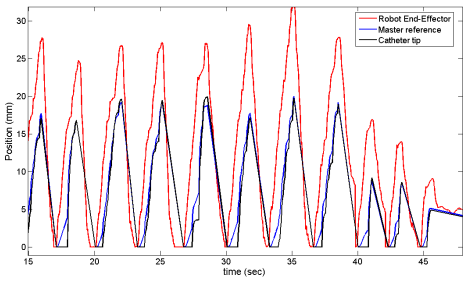

Fig. 7. Magnified view of normal insertion in region (a) of Figure 6

VII. Conclusion

In this paper, we have developed a bilateral teleoperation framework to perform robot-assisted active catheter insertion. The tip of the catheter very closely follows the motion of the haptic device while the forces at the tip are reflected to the master. In addition, we have shown in the paper that the robot end effector moves up to nearly 600% more than the tip of the catheter in order to compensate for the flexing in the catheter. By controlling the tip of the catheter (instead of the robot end-effector) as the slave, the clinician is provided with a more transparent procedure, wherein the tip of the catheter very closely follows the motion of the master. In this paper, we have also studied various factors influencing the flexing in the catheter. These results should help in developing a more accurate model for the flexing of the catheter and aid in improving the accuracy of master-slave catheter insertion for applications in angioplasty and cardiac ablation.

References

[1] M. Kukuk and B. Geiger, "A real-time deformable model for flexible instruments inserted into tubular structures," in *MICCAI '02: Proceedings of the 5th International Conference on Medical Image Computing and Computer-Assisted Intervention-Part II*. London, UK: Springer-Verlag, 2002, pp. 331–338.

[2] J. Lenoir, S. Cotin, C. Duriez, and P. Neumann, "Physics-based models for catheter, guidewire and stent simulation," in *Medicine Meets Virtual Reality (MMVR)*, Long Beach (CA) - USA, January 24-27 2006, pp. 305–310.

[3] A. Theetten, L. Grisoni, C. Duriez, and X. Merlhiot, "Quasi-dynamic splines," in *SPM '07: Proceedings of the 2007 ACM Symposium on Solid and Physical Modeling*. New York, NY, USA: ACM Press, 2007, pp. 409–414.

[4] M. Azizian, J. Jayender, and R. V. Patel, "Image processing algorithms for real-time tracking and control of an active catheter," in *European Control Conference (ECC)*, 2007.

[5] A. Kazi, "Operator performance in surgical telemanipulation," *Presence*, vol. 10, pp. 495–510, 2001.

[6] G. Niemeyer and J. J. E. Slotine, "Telemanipulation with time delays," *International Journal of Robotics Research*, vol. 23, pp. 873–890, 2004.

[7] R. J. Anderson and M. W. Spong, "Bilateral control of teleoperators with time delay," *IEEE Transactions on Automatic Control*, vol. 34, pp. 494–501, 1989.

[8] J. Jayender, R. V. Patel, and S. Nikumb, "Robot-assisted catheter insertion using hybrid impedance control," in *2006 IEEE International Conference on Robotics and Automation (ICRA)*, May 2006.

[9] H. Seraji, "Configuration control of redundant manipulators," *IEEE Journal of Robotics and Automation*, vol. 5, pp. 472–490, 1989.

[10] L. A. Eisen, T. Minami, H. Sekiguchi, J. S. Berger, P. Mayo, and M. Narasimhan, "Ultrasound demonstration of asymmetry between the left and right femoral and radial arteries," *Chest*, vol. 103, pp. 201S–a, 2006.

[11] Y. Ikari, M. Nagaoka, J.-Y. Kim, Y. Morino, and T. Tanabe, "The physics of guiding catheters for the left coronary artery in transfemoral and transradial interventions," *The Journal of Invasive Cardiology*, vol. 17, pp. 636 – 641, December 2005.